

# Airbag Simulation with LS-DYNA Past – Present – Future

A. Hirth<sup>1</sup>, A. Haufe<sup>2</sup> & L. Olovsson<sup>3</sup>

<sup>1</sup> DaimlerChrysler AG, EP/SPV, HPC 059-X276, D-71059 Sindelfingen, Germany

<sup>2</sup> Dynamore GmbH, Industriestraße 2, D-70565 Stuttgart, Germany

<sup>3</sup> IMPETUS Afea AB, Norrbyvägen 58, SE-141 30 Huddinge, Sweden

## 1 ABSTRACT

During the last decade the simulation of the airbag deployment process has become a standard application of explicit finite element codes. At the beginning of the development the focus was to capture the influence and improve the results of dummy impact on fully inflated airbags. Later the deployment kinematics of folded airbags, different folding techniques and vent-hole design became more and more important. With the requirement to comply with FMVSS 208, i.e. Out-of-Position load cases, it became apparently necessary to include the interaction between the internal gas flow and the fabric airbag structure. Hence coupled algorithms that allow for interaction between the discretized gas flow and the airbag structure were the main focus during the past five years.

The present paper aims to sketch the development history of airbag deployment simulations from the very beginning of the late 1980s to the current, highly sophisticated models available in LS-DYNA. Different modelling techniques will be shown and their advantages, drawbacks and the necessary effort to gain useful results will be discussed.

### KEYWORDS:

Airbag deployment simulation, uniform pressure, Fluid-Structure-Interaction, Arbitrary-Lagrangian-Eulerian method, corpuscular (particle) method

## 2 Introduction

During the last decade the simulation of the airbag deployment process has become a standard application of explicit finite element codes. At the beginning of the development the focus was to capture the influence and improve the results of dummy impact on fully inflated airbags. Later the deployment kinematics of folded airbags, different folding techniques and vent-hole design became more and more important. With the requirement to comply with FMVSS 208, i.e. Out-of-Position load cases, it became apparently necessary to include the interaction between the internal gas flow and the fabric airbag structure (see [1], [2], [3] and [4]). Hence coupled algorithms that allow interaction between the discretized gas flow and the airbag structure were the main focus during the past five years. A general and also for other applications successful and suitable approach is to discretize the gas domain with finite elements and hence capture flow and deformations with the ALE method. Interaction between gas and airbag fabric is handled with either penalty or constraint formulations.

At the same time of course, the typical element size decreased, the total amount of elements increased and further sophistications in constitutive laws, reference geometry handling and porosity consideration etc. were included in the code. Clearly, all of this accumulated more and more complexity to the every day airbag simulation workload. Moreover, with the newest releases of LS-DYNA 971 a sophisticated and very promising particle based method will be available.

In the present paper the authors will sketch the development of airbag modelling techniques starting from the beginning of the 1990s until today. The uniform pressure technique, ALE method and the recently developed corpuscular particle method will be covered. Results as well as advantages and disadvantages of each method will be presented and discussed in the context of different applications. Recommendations towards which method to use in specific applications will be given.

## 3 Prerequisites to gain reliable airbag simulations

In order to gain reliable and predictable airbag simulations a sufficient basis of test data for the airbag fabric is necessary. However, without having a suitable constitutive model in the corresponding FE code at hand even the largest amount of test data is useless. Besides the standard static and dynamic tension test, so called picture frame tests and biaxial tests, where a patch of the fabric in question is loaded in pure shear and biaxial tension, respectively, are investigated (see Figure 1). From such tests corresponding true stress – true strain curves as depicted in Figure 2 are obtained. The tests build the basis of the subsequent validation procedure that will be discussed in the following.

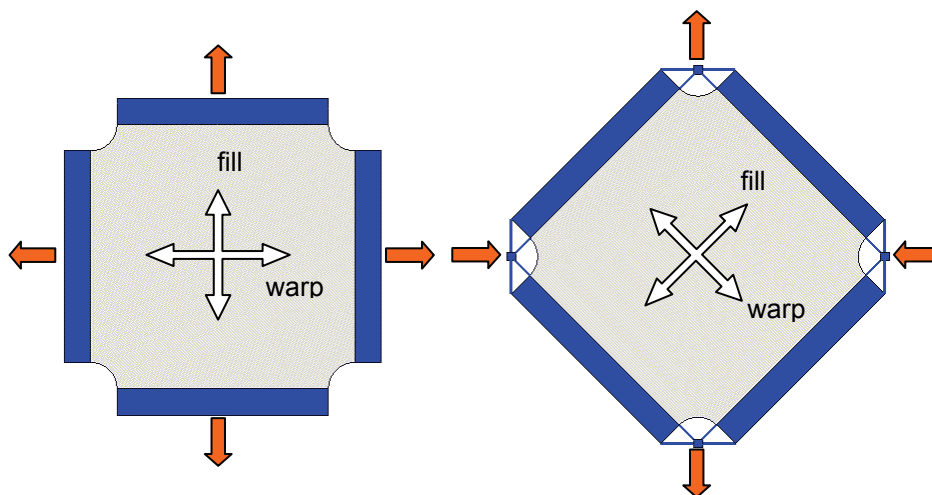


Figure 1: Biaxial tension and picture frame test

In LS-DYNA MAT\_FABRIC (#34) is intended for use in airbag applications. During the development process from the very beginning, the underlying constitutive model has evolved from a rather simple bi-linear orthotropic model to the latest implementation with nonlinear biaxial loading and unloading curves. For shear loading and unloading curve definitions are available also, as well as curve input for porosity. This development process is documented in the increasing number of formulations that can

be seen in the parameter FORM. While the earliest formulation starts with FORM=0, the latest and most advanced formulation is available with FORM=14. Here LS-DYNA expects true stress – true strain data in a number of input curves. It is obvious though, that these curves need to be extracted from adequate tests. In addition the younger models (FORM=4/14) allow also definition of non-orthogonal material axes.

In Figure 2 test data of a biaxial tension test and a picture frame test are depicted (black curve with round dots). The test data was evaluated, stress and strain computed and used within a validation procedure that was based on a detailed discretization of the test setup. It can be seen, that the older formulation FORM=0 is not able to capture neither the loading nor the unloading behaviour in a suitable way. The much younger formulation FORM=4, that not only expects nonlinear loading but also unloading curves is able to capture the biaxial behaviour good enough. However, as can be seen in comparison to the picture frame test data, FORM=4 delivers a great amount of unphysical oscillations. Only the latest development FORM=14 which is enhanced by a special treatment of the shear data is able to predict the biaxial and picture frame test data suitable. Also it must be noted that in order to predict the biaxial test correctly, curve data from biaxial tests has to be used instead of data from pure tension tests. Otherwise the first hump in the test data, due to interaction of warp and fill threads and subsequent stiffening, will not be reproduced.

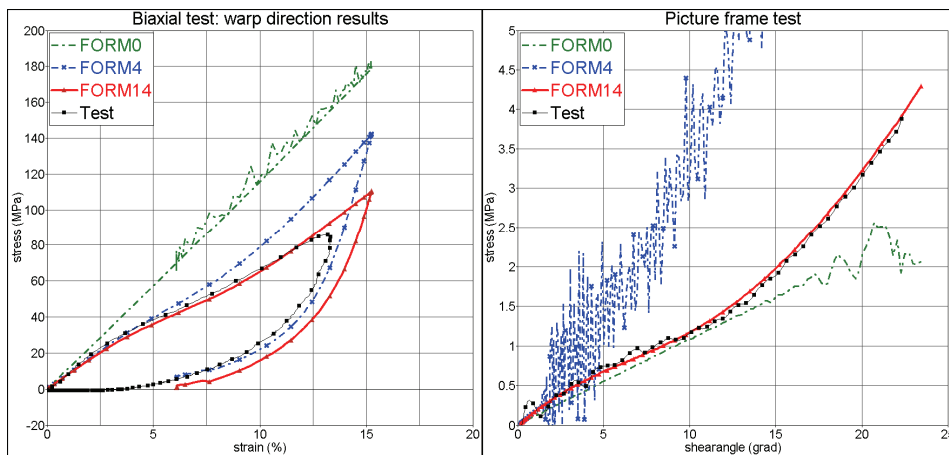


Figure 2: Biaxial tension and picture frame test

## 4 Overview on airbag deployment algorithms in LS-DYNA

### 4.1 UNIFORM-PRESSURE (UP)-Technique

The simulation of the deployment process of an airbag system was first performed with FE-Methods simulating the dynamic behavior of the system by explicit time-stepping schemes. These explicit methods are especially suited for such complex, highly nonlinear systems because of their complicated contact situations during the deployment from an initially folded configuration. As rough approximation of the time-dependent behavior of the interior pressure of the bag the so-called uniform pressure technique was developed in the late 1980s by Wang and Nefske [9], see also Figure 3a.

In any time step the volume of the airbag is being calculated by applying the Gaussian integral theorem. Assuming an ideal gas law and an adiabatic process, pressure can be determined as a function of density  $\rho$  as:

$$p = (\gamma - 1) \rho e \quad (1)$$

Here  $\gamma$  is the isentropic coefficient  $c_p/c_v$  and  $e$  the specific internal energy ( $e = E_{\text{int}} / \rho_0$ ). For two neighboring states of deformation denoted with subscripts 1 and 2 there is:

$$\frac{e_2}{e_1} = \left( \frac{V_1}{V_2} \right)^\gamma = \left( \frac{\rho_2}{\rho_1} \right)^\gamma \quad (2)$$

With this equation from a known volume  $V_2$  at a time step  $t=t_2$ , the volume at the previous time step  $V_1$  and the appropriate internal energy  $e_1$  the actual internal energy  $e_2$  can be determined. From the internal energy the pressure can be calculated and applied as pressure load normal to the entire airbag fabric. For the deployment process itself the method must be further extended. The inflating gas is given by a time dependent mass flux  $\dot{m}_{12}$  with an appropriate inflow temperature of the gas. Due to Wang and Nefske (see [9]) the total inflating mass flux is split into three components (see Figure 1):

$$\dot{m}_{tot} = \dot{m}_{in} + \dot{m}_{out} = \dot{m}_{12} + \dot{m}_{23,vent} + \dot{m}_{23,porosity} \quad (3)$$

Here  $\dot{m}_{23}$  stands for the mass loss due to vent holes and porosity of the airbag. The expression for the internal energy increase due to gas entering and leaving the bag may be written:

$$\dot{E} = c_p (\dot{m}_{in} T_1 + \dot{m}_{out} T_2) - p \dot{V} \quad (4)$$

The actual values for pressure are being determined in a similar way to eqn. (1).

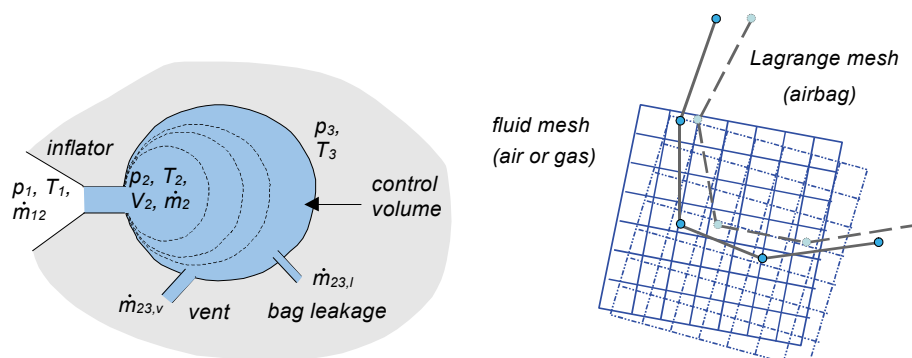


Figure 3: a) Uniform pressure concept  
b) ALE mesh movements at two adjacent time steps

Summarizing one can note that for the UP-technique there is no discretization of the fluid flow. The whole concept is based upon scalar thermodynamic equations. Extensions, which take into account a dependency of the pressure field on the inflow direction (commonly termed jet) are based on the same simple assumptions. It is also possible, to take into account a gas mixture (so-called hybrid gas generators) or temperature-dependency of the specific heat coefficients. The calculation time can be neglected in comparison to the calculation time necessary for the structural behavior of the airbag. The inflow values (mass fluxes and temperature values over time) are usually determined by tank tests in combination with additional techniques to estimate the temperature.

At this point it is important to mention the main deficiency of this traditional airbag deployment approach: It is a strongly simplified model of the process especially neglecting local fluid effect. While this is only of minor importance in a regular case, where the dummy or passenger is hit by the airbag in a situation, where the airbag is already almost fully deployed, the situation is different in an OoP-load-case. Here the dummy or passenger is in contact with the airbag in a much earlier stage of the deployment process and a physically correct model of the flow situation is necessary. The same holds for studies of deployment sequences as for instance necessary for curtain bags.

#### 4.2 The Arbitrary-Lagrangian-Eulerian (ALE) approach to airbag deployment simulations

To model the gas dynamics correctly a discretization of both, the air volume surrounding the airbag and the inflowing gases, and the coupling forces is needed. A very elegant mathematical description of both field equations can be performed through the Arbitrary- Lagrangian- Eulerian-(ALE)-concept (see [6] and [7]).

In the ALE-concept, as indicated by its name, an arbitrary approach that allows mixture of Eulerian and Lagrangian description is used. In a Lagrangian system the observer will move with the material while in a pure Eulerian description the observer is fixed in space and the material points are moving through a stationary grid of fixed points. In an ALE based approach the observer may follow its own

arbitrarily defined path in space. It is obvious, that the two extreme cases of the more general ALE-method come down to the classical description of the Eulerian grid, which is commonly used in pure flow problems and the pure Lagrangian description, which is commonly used in structural problems. Mathematically an arbitrary reference domain leads to an additional term in the conservation laws. In the numerical algorithm an additional set of equations must be solved, as the dynamics of the moving grid points has an impact on the discretized problem, which is being shown in Figure 3b. In the following the conservation laws are being given. The whole set of equations is solved inside LS-DYNA by an explicit time-stepping algorithm. The additional terms due to the grid movement are highlighted by a separate color inside the dashed box:

$$\text{Momentum conservation} \quad \rho \ddot{\mathbf{x}} + \rho \nabla \dot{\mathbf{x}}(\mathbf{v} - \dot{\mathbf{x}}) = \rho \mathbf{b} + \text{div } \boldsymbol{\sigma} \quad (5)$$

$$\text{Mass conservation:} \quad \dot{\rho} + \nabla \rho(\mathbf{v} - \dot{\mathbf{x}}) + \rho \text{div } \mathbf{v} = 0 \quad (6)$$

$$\text{Energy conservation:} \quad \rho \dot{\mathbf{u}} + \rho \nabla \mathbf{u}(\mathbf{v} - \dot{\mathbf{x}}) = \boldsymbol{\sigma} : \mathbf{D} + \rho \mathbf{r} - \nabla \mathbf{q} \quad (7)$$

Within these equations  $\mathbf{v}$  denotes the material velocity and  $\dot{\mathbf{x}}$  the velocity of the grid points.  $\rho$  denotes the density,  $\mathbf{b}$  external body forces and the last two terms in equation (7) denote heat sources and sinks.  $\mathbf{D}$  represents the constitutive tensor.

For this simplified description, we must note, that equations (5) to (7) in the case of an ALE description are referencing to an ALE-coordinate system. If the highlighted terms are deleted, a Lagrangian system is referenced. If  $\dot{\mathbf{x}}$  is set to constant zero the pure Eulerian system is referenced.

As usual in the Eulerian approach also in a “moving” Eulerian approach mass transport between elements has to be taken into account. This so-called advection must be treated in a special way within the numerical algorithm to ensure stability and accuracy of the numerical scheme. In LS-DYNA a first order (Donor cell scheme) and second order (Van Leer’s scheme) accurate flux vector splitting scheme is available. For the Multi-Material-ALE-Formulation up to eight different materials with the appropriate history and state variables have to be taken into account by the advection scheme (see [7] and [8]). Furthermore for hybrid airbags a gas mixtures model has been implemented, due to the high demand to integrate hybrid gas generator data as commonly used for UP-based airbag simulations. Another aspect concerning the accuracy achieved during the advection step is related to the allowed maximum time step size. To get a sufficiently accurate and stable scheme, the material flux within one time step is limited to a quarter of the element size, which means that the mass flux relatively to the grid movement determines an additional time step limiting criterion to the existing Courant-criterion arising from the explicit time-stepping scheme.

Besides the gas dynamic effects the unfolding of the airbag leads to another algorithmic challenge that needs to be considered also. The airbag is being discretized in the classical Lagrangian approach. The missing link between the two different discretization schemes must be handled by an appropriate coupling mechanism, which solves the interaction problem between the gas and the airbag fabric. For airbags special version of a penalty-based coupling scheme is recommended. This method applies a so-called penetration vector, which represents the intrusion of the gas into the surrounding air volume thereby moving through the airbag fabric. A pressure-penetration-relationship is defined, which determines the penalty-force that will push the gas material back into the airbag.

Nowadays in a passenger car both coated and uncoated airbags are being used. In the case of uncoated porous fabrics the classical uniform-pressure-concepts come with special empirically determined terms to account for the mass loss due to the porosity of the airbag fabric. As the ALE-concept does not contain the possibility of real (porous) flow through the airbag and the algorithm tries to avoid artificial leakage effects, the wish to account for porosity effects contradicts these goals. Therefore in LS-DYNA the mass loss due to the flow through the airbag is subtracted from the system. This is being implemented by experimentally determined curves, which describe the gas velocity through the airbag fabric as a function of pressure difference between in- and outside the airbag volume. In the conservation laws the kinetic energy loss is balanced by an additional heat source.

### 4.3 Corpuscular (C) method for airbag deployment simulations

#### Basic concept

The static gas pressure in a volume  $V$  is a direct function of the total translational kinetic energy of the molecules in the gas. The pressure  $p$  is built up by molecules colliding with the boundary of the volume.

$$\text{Kinetic energy: } p = \frac{2}{3} \frac{W_k}{V} \quad (8)$$

$$\text{Molecular mass \& velocity: } W_k = \frac{1}{2} \sum_{N_m} m_i v_i^2 \quad (9)$$

There are typically  $10^{23}$ - $10^{24}$  molecules in an inflated airbag and one can not treat each and every one of them individually in a numerical model. That is why one normally reverts to a continuum treatment of the gas and to numerical methods such as FEM, SPH or EFG. However, a continuum treatment of the gas creates geometrical difficulties in the gas-fabric contact and in the handling of gas flow through narrow gaps (see Figure Figure 4a).

The new method in LS-DYNA for airbag simulations is unique in that it stays with a corpuscular modeling of the gas flow. That is, the gas is modeled as a set of individual particles. This has been made possible by letting each particle represent many molecules (see Figure 4b). The expected pressure is matched by ensuring that the total translational kinetic energy of the particles is correct.

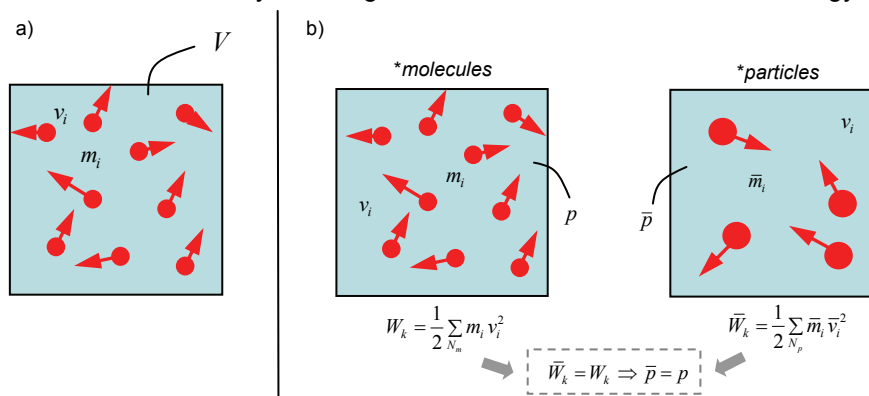


Figure 4: a) Particle approach b) Particle vs. Molecule description

Note that the particles, just like molecules, can store some energy as spin and vibrations. This is necessary for a correct ratio between  $C_p$  and  $C_v$  and, hence, also for a correct behavior of the gas during expansion/compression.

Assigning the particles the same properties as molecules in classical gas theory, one automatically matches the pressure drop in adiabatic expansion ( $pV$ -work).

$$\frac{dp}{dV} = -\frac{C_p/C_v}{V} p \quad (10)$$

#### Limitations

Deviations from thermal equilibrium are not treated entirely perfectly, but seemingly well enough for airbag analyses. One also has to make sure that the number of particles is not too low, the number depends on the volume that has to be filled. In paragraph 5.2 this issue will be investigated in detail.

### Porosity, vent holes and blockage

Porous properties are taken directly from \*MAT\_FABRIC (FLC and FAC curves) as usual for UP and ALE bags. Vent holes must be modeled physically as patches of shell elements. This is necessary for a correct bag volume calculation and for a correct treatment of the external atmospheric pressure (generally 1bar). Blockage can be taken into account (both venting and porous flow), by setting a flag in the input deck.

## 5 Comparison of UP, ALE and C - method

In the following some airbag examples are present where the specific advantages and drawbacks of each method are shown.

### 5.1 Example 1: Comparison of methods exemplified at flat airbag with perpendicular inflow

The first example shows a square unfolded airbag. The bag is inflated by an inflator (with two separated mass flow curves, constant temperature, see Figure 5) with the UP (\*AIRBAG\_HYBRID\_JETTING), the ALE (\*AIRBAG\_ALE with 27 000 cells) and the new C method (\*AIRBAG\_PARTICLE with 10 000 particles). In order to get comparable results the jetting option for the UP inflator was used. In the present example we only investigate the qualitative results, i.e. the shape of the bag at certain time steps. Experimental results are not available. In Figure 7 different shapes of the airbag deployed with all three methods are shown at different time steps.

It can be seen that all three methods lead to approximately the same result. The shapes and also the energy introduced into the bag do not differ significantly, see also Figure 6. The slight geometrical deviations are attributed to the shape of the inflow stream, which is different in each method due to different discretization (ALE and C method) or pure velocity profile assumptions at all (UP jetting).

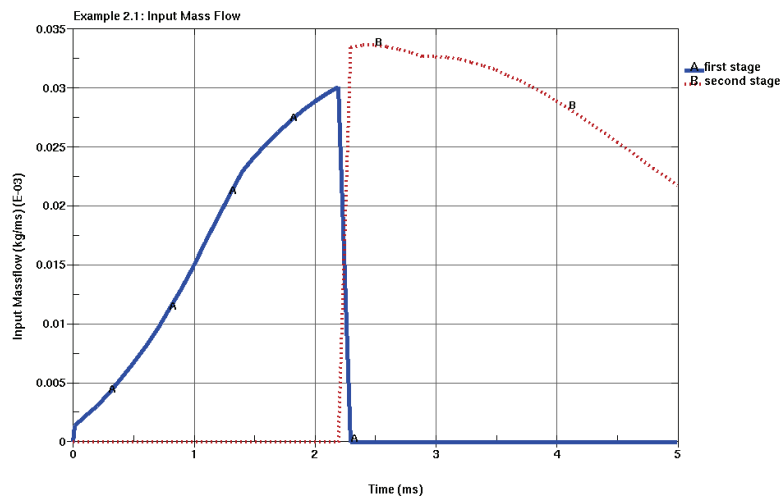


Figure 5: Separated mass flows for inflator

The only point that needs to be mentioned is the fact that the C method seems to be slightly more sensitive to inflow variations. This may be also the reason for the slight perturbation of the internal energy of the C method as depicted in Figure 6 (right diagram, blue curve). It is of minor importance though.

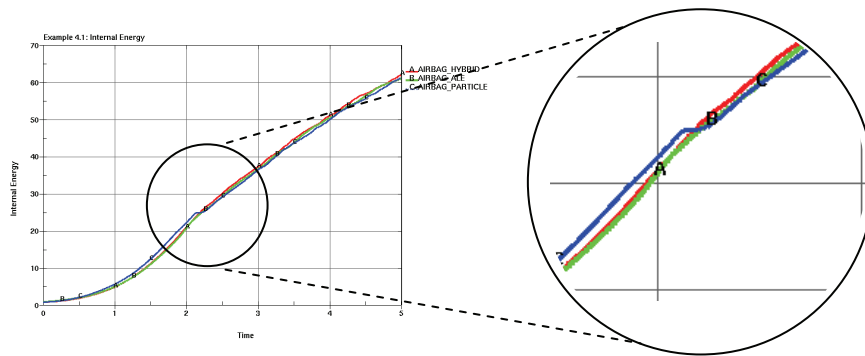


Figure 6: Detailed view of internal energy at switching to second mass flow

time	*AIRBAG_HYBRID JETTING	*AIRBAG_ALE	*AIRBAG_PARTICLE
0 ms	jetting vector 		
1 ms			
3 ms			

Figure 7: Shape of airbag with different deployment simulation methods

Computing time for the different methods is as follows: UP: 21 sec, ALE: 2010 sec and C: 161 sec on SMP machines (AMD 2.8 GHz). Hence, in terms of computing time the new C method outperforms the ALE method by a factor of 12. Clearly, this is strongly dependent on the ALE mesh size and the number of particles used but gives a general impression that will be backed up by the following examples.

## 5.2 Example 2: Comparison of methods exemplified at flat airbag with inclined moving inflow vector

The second example is identical to example 1 except for the following changes: Now a vent hole is modelled and the inflow is defined through a spinning jet vector that is inclined by  $60^\circ$ , see Figure 8. Furthermore, a fourth simulation run is set up for this example. Here again the ALE method is applied, where in contrast to the previously used \*AIRBAG\_ALE keyword, the input deck is built up by individual ALE-cards. This approach is much more troublesome but give a great amount of control and more flexibility compared to the simple, yet in most cases sufficient \*AIRBAG\_ALE-card. The setup with individual ALE-cards will be termed "Common ALE" in the following.

Obviously the spinning inflow jet cannot be modelled with the available UP method in LS-DYNA. The same holds for the simple \*AIRBAG\_ALE-card. Hence stronger deviations of these two methods from the other two discretization methods are expected. Also, the number of particles has been increased to 50 000, in order to capture the hole and the spinning effect of the jet realistically.

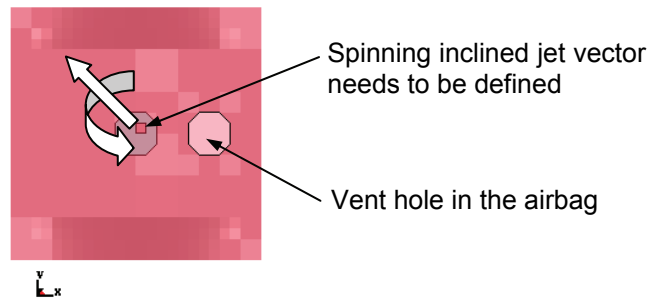


Figure 8: Setup of second example

As can be seen from the pictures in Figure 10 the UP approach delivers a homogeneous deflation only due to the lack of spin of the jet vector, while the mass flux through the vent hole is very similar compared to the C method (\*AIRBAG\_PARTICLE), see Figure 9a. The difference is explicable since in UP the vent hole acts from the beginning, while for the C method the hole might be covered and hence blocked for the first microseconds. Also Figure 9b shows good correlation of airbag pressure between UP and C method.

Furthermore the differences between \*AIRBAG\_ALE and the common ALE approach are seen in Figure 10 as expected. For \*AIRBAG\_ALE no spinning of the inflow vector is possible, hence the inflation looks quite unrealistic. Here the same holds as for the UP method. Also, the vent definition in \*AIRBAG\_ALE is based on internal removal of gas - no visualization of the gas leaving the airbag is possible.

Only the common ALE approach and the C method allow for the spinning of the inflow vector. In addition with these two methods visualization of the outflow through the vent hole is possible. It should be noted though, that the outgoing mass flux is strongly dependent on the Eulerian mesh size. If the outflow is believed to be too little, the whole input needs to be reworked, since not only a finer Eulerian mesh needs to be defined, but also the airbag mesh must be refined accordingly. Otherwise validated curve data and leakage parameters in the constraint card(s) need recalibration which is rather time consuming.

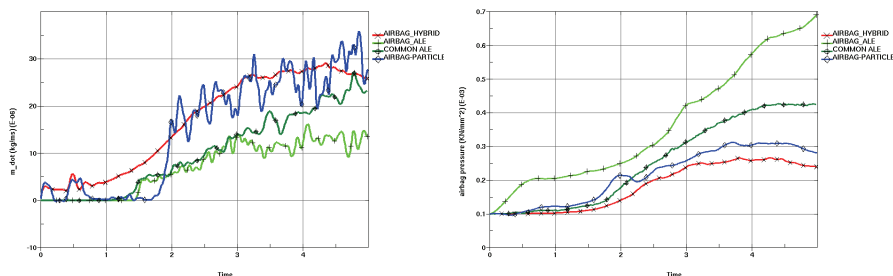


Figure 9: a) outgoing mass flux b) airbag pressure

Furthermore with \*AIRBAG\_ALE and Common ALE it is possible to visualize all relevant flow information like pressure or velocity distribution in the airbag. Currently these features are still missing for the new C method. However, it is believed that within a short amount of time the lacking visualization features will be added to LS-PrePost.

Finally SMP-computing time for all four methods need to be compared. It is again obvious that the UP method with 21 sec. is the fastest followed by the C method with 372 sec. The ALE approaches deliver their results slower: 3148 sec. A factor of about 9 in favour of the particle is experienced.

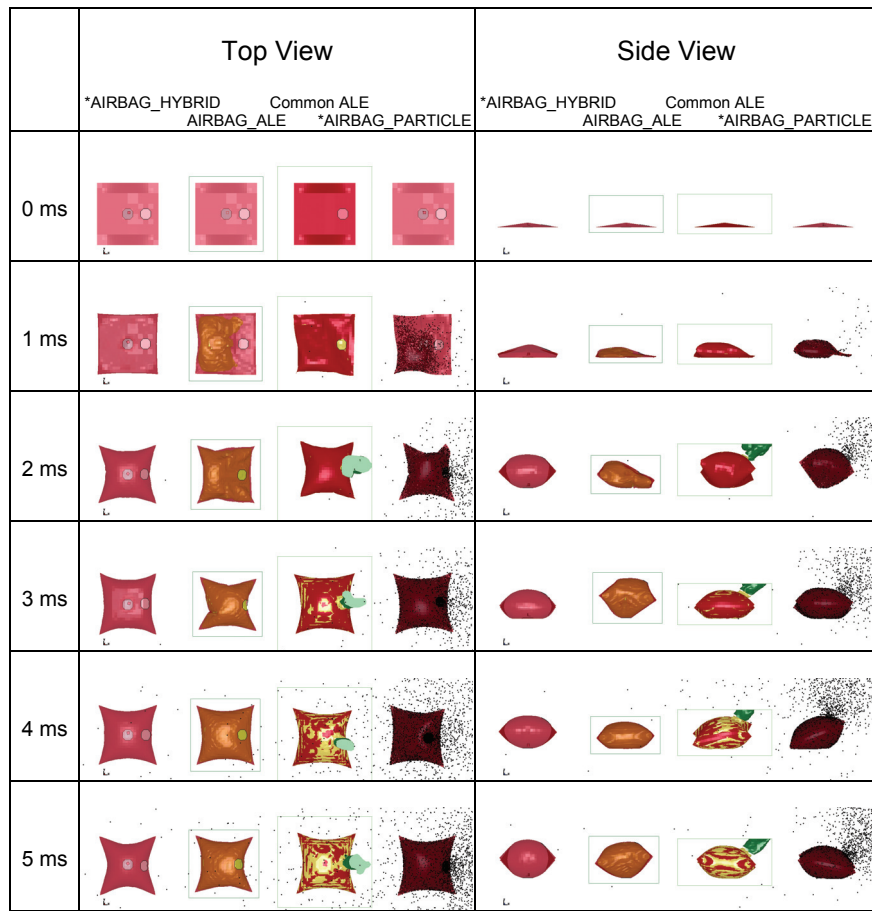


Figure 10: Top and side views at different stages of the simulation

### 5.3 Example 3: Multiple chamber problem

The following example shows a principal problem experienced with the ALE. For this problem three different methods have been applied: A UP inflator, the common ALE-methods with 112 000 cells and the C method with 50 000 particles.

Due to the fact that the ALE modelling technique needs to constrain the Eulerian discretized gas within the Lagrange discretized airbag, the forces acting on both node groups (Eulerian mesh and Lagrangian mesh) are calculated on a penetration basis. This works flawlessly in many situations. However, when a folded bag gets pressure from both sides, the underlying algorithm generates of course forces from both sides as well. This can lead to unphysical behaviour when two airbag patches lie parallel within one Eulerian cell. An example for the delivered behaviour is a flat window bag, that when fully opened consists of tubes under high pressure contacting each other. Here the ALE-method does not lead to a physically correct shape of the tubes as can be inspected in Figure 11. Contact penetrations that make one fabric patch stuck in the other patch are observed, see Figure 12.

For the sake of completeness the simulation times (SMP) are given as follows: The UP method delivers results after 640 sec, the ALE methods after 5 572 sec and the new C method after 4 054 sec. Here it can be seen that the advantage of the C method decreases as the number of particles and the total problem size increases. This trend can be observed in general. But then, at present a fully operational MPP implementation of the method is still under development. Hence significant speed up is expected in future also for larger input decks and larger particle numbers.

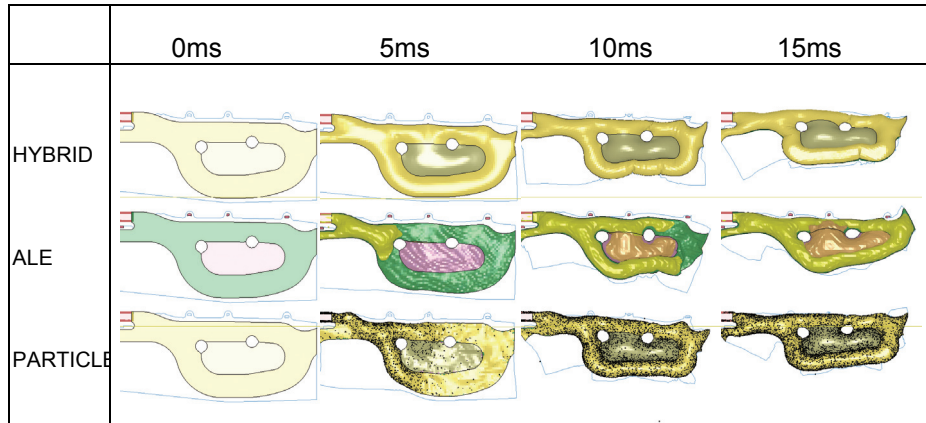


Figure 11: Multiple chamber airbag deployment study

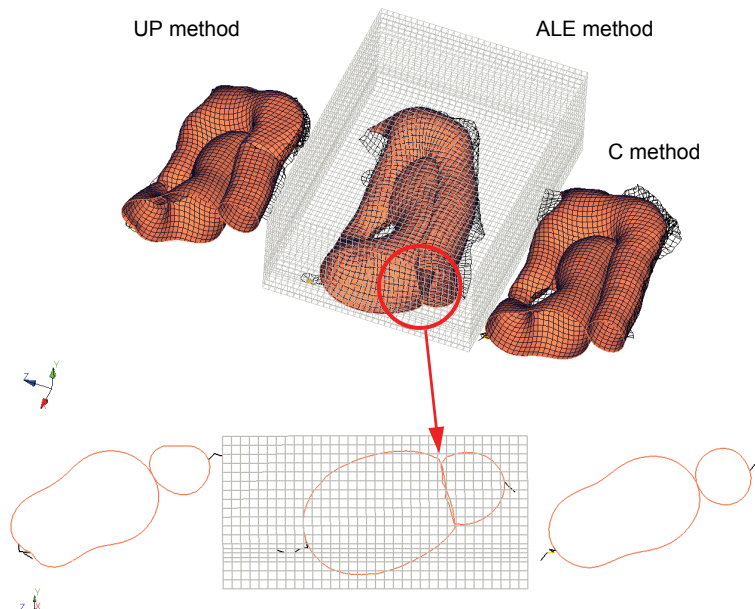


Figure 12: Detail of airbag chambers and cross sections at 10 ms

#### 5.4 Example 4: Small fabric tube problem

Another very challenging task during airbag deployment is to open up a tightly folded fabric structure. Clearly, the uniform pressure approach manages this task very easily due to the fact that the actual pressure is applied uniformly to all faces. As long as the contact handling manages the situation no problems should occur. For a fluid-structure-interaction driven approach the same task may be a bit harder. Here the opening of individual folds is driven by the action of the gas on the fabric face. Hence opening is not taking place at all faces at the same time but consecutively along the folded structure. This requires a sufficiently fine discretization of the fluid and the Lagrangian fabric structure.

It was shown in [1] that the ALE-method in LS-DYNA is capable of simulating the deployment of such structures. However, it was also noticed by the authors, that a certain fineness of the Eulerian mesh was necessary to successfully capture the effect. Hence computing time was very large even on fast clustered computers. It is anticipated that the C method, due to the fact that the individual particle should open up the folds very easily, shows a much better behaviour with a less fine discretization of the gas and less computing time.

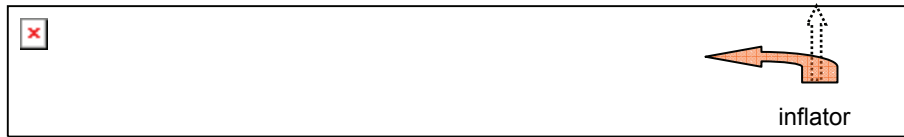


Figure 13: Cross section cut of tube problem

In the following a twice folded tube is deployed with three different methods: A standard UP inflator with the \*AIRBAG\_HIBRID keyword, the ALE-method with 176 000 Eulerian elements and the C method with 50 000 particles. Particularly the ALE discretization should be fine enough to capture the fold. Here, the ALE domain is defined to grow in size with the inflating structure. The airbag model is depicted as cross section cut in Figure 13 and the deployment study of all three methods is shown in Figure 14. It is shown that all three methods deliver totally different deployment histories of the tube problem. Also, due to the completely different deployment process and thereby developing different structural dynamic the final geometry state is quite different.

Especially in columns 2 and 3 in Figure 14 a remarkable difference between the ALE method and the C method can be seen. Here the ALE method opens up the tube one element row by another since the fluid can not reach any region upfront before the tube has opened to a certain level. The C method however is able to "send" some particles through even tight folds which subsequently help opening the bag from both sides. Whether one or the other method shows a more physical behaviour remains to be discussed and validated by appropriate experimental studies. However, it is assumed that the opening speed of the ALE method is too low compared to reality, hence a better agreement of the C method with the experiment is expected.

Finally it should be mentioned that again the C method shows a shorter computing time of factor 7 compared with the ALE method. While the UP method takes 205 sec and the C method takes 5858 sec. the ALE method takes 42 429 sec. on SMP machines.

	*AIRBAG_HYBRID	*AIRBAG_ALE	*AIRBAG_PARTICLE
0ms			
5ms			
10ms			
15ms			
20ms			

Figure 14: Deployment study of tube problem

## 6 Application in engineering practise: Comparison with experimental studies

### 6.1 Flat driver airbag problem

In this study the deployment of a flat unfolded driver airbag is simulated. Again three different simulation methods are compared. In addition detailed experimental results are available that allow validation of each model against reality. The airbag consists of about 32 000 elements where the characteristic element size is about 4mm. The total airbag volume is 60 litres which is inflated by a typical one stage inflator. Inside the bag a deflator is installed to deflect the flow direction from the horizontal outflow holes to a more vertical direction, see Figure 15. A semi-sphere with a mass of 15 kg is located in front of the airbag and will be impacted and accelerated by the deploying airbag. The airbag has no vent holes and the fabric is not porous. Moreover 100 % of the inflator generated energy is used in the input curves for mass flow and temperature. Particularly a typical scaling of the inflow temperature which is common for validation procedure for UP models is not done. Again one model is set up with \*AIRBAG\_HIBRID, another one with the ALE-method consisting of 350 000 Eulerian elements and the last one is set up with 250 000 particles.

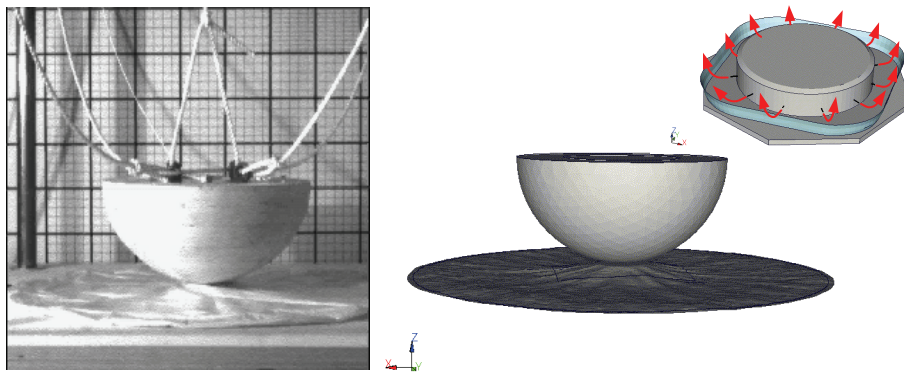


Figure 15: Test setup, corresponding airbag, impactor and deflator finite element model

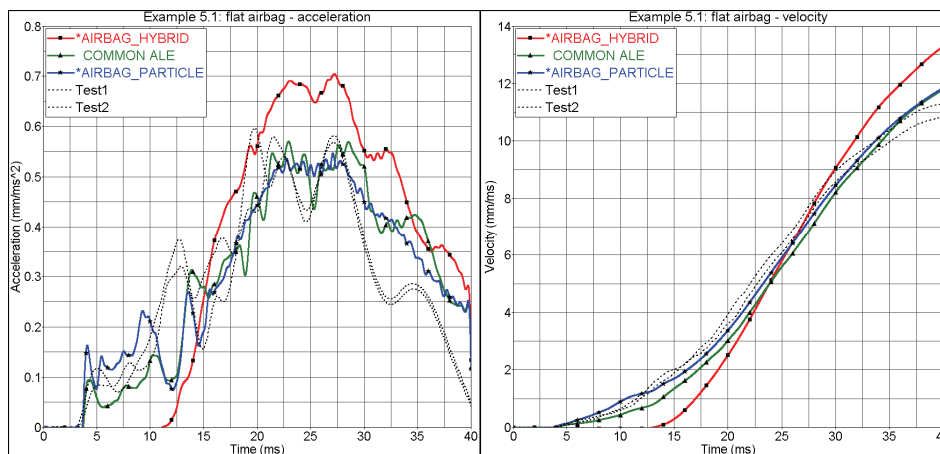


Figure 16: Acceleration and velocity of the semi-sphere compared to test data

In Figure 16 the simulation results in terms of acceleration and velocity of the semi-sphere are shown. It can be seen that the results with the UP approach underestimate the experimental data at the beginning and overestimate the behaviour at the end. Since the test setup was chosen to resemble an out-of-position load case, where the drawbacks of the UP method are known, these results were expected. The ALE and the C method show a good correlation in this experiment.

In terms of computing time the UP run took 2.546 sec SMP on an AMD 2.8GHz computer, the ALE run took 110.050 sec and the C method finished after 13.584 sec on the same hardware.

## 6.2 Folded driver airbag problem

This example is set up identical to the previous one with one distinctive difference: Now the airbag is folded, see Figure 17. Also, for this model a detailed investigation on the number of particles, i.e. a convergence study for \*AIRBAG\_PARTICLE, and a comparison for the methods on SMP and MPP machines is presented.

Acceleration and velocity plots of the semi-sphere are given in Figure 18 for all three investigated modelling techniques. It can be seen that without additional modifications to the input parameters the UP method underestimates the first acceleration peak and overestimates the remaining acceleration data. The same trend for UP has been seen in example 5.1. For both, ALE and C method, the results correspond very well with the test data. It must be mentioned though, that for such a good correlation all other sensible parameters in the model, i.e. internal friction of the folded airbag fabric, friction between fabric and sphere, material parameters and constitutive formulation as discussed earlier need to be validated rigorously.

In Figure 19 the results of the convergence study for the C method is depicted. Again, acceleration data as well as velocity data is plotted against the corresponding test results. It can be seen that there exists a lower bound for the number of particles. While 50 000 and 100 000 particles seem to be not enough for the present problem, increasing their number to about 250 000 particles leads to perfect results in terms of validation acceptance. The differences in the results between 250 000 and 500 000 particles are minor. Clearly, increasing the number of particles has an impact on the computing time, which can be investigated in Figure 21. In addition Figure 20 shows the computing time of UP, ALE and the C method on SMP machines. While ALE on SMP machines is by a factor of 15 slower than UP, the same task solved with the C method shows only a time increase of factor 3 when compared to UP. Hence \*AIRBAG\_PARTICLE is 5 times faster than ALE on the same SMP hardware.

As remark one may add that for the ALE-Method the time step is in most applications controlled by the smallest solid element of the Eulerian mesh. Hence the time step condition leads usually to much smaller time steps than for the other two methods. For both \*AIRBAG\_HYBRID and \*AIRBAG\_PARTICLE the step size is only controlled by the Lagrangian elements of the bag.

Concerning the MPP simulation times compared in Figure 22 a clear speedup is noticeable and feasible. It should also be mentioned that the speed up of the C method is already significant from 1 to four processors – any higher number of processors does not - at present - result in shorter total computing time. Further development is under way. Clearly, all MPP runs lead to identical results.



Figure 17: Test setup and corresponding finite element model

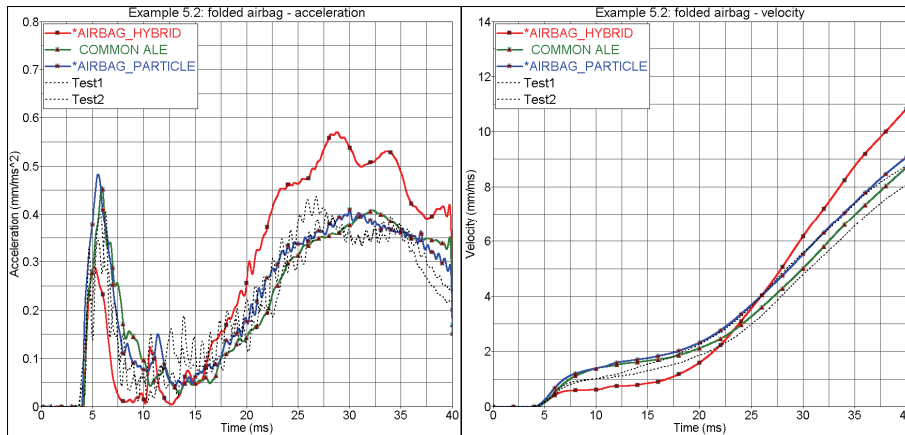


Figure 18: Acceleration and velocity of the semi-sphere compared to test data

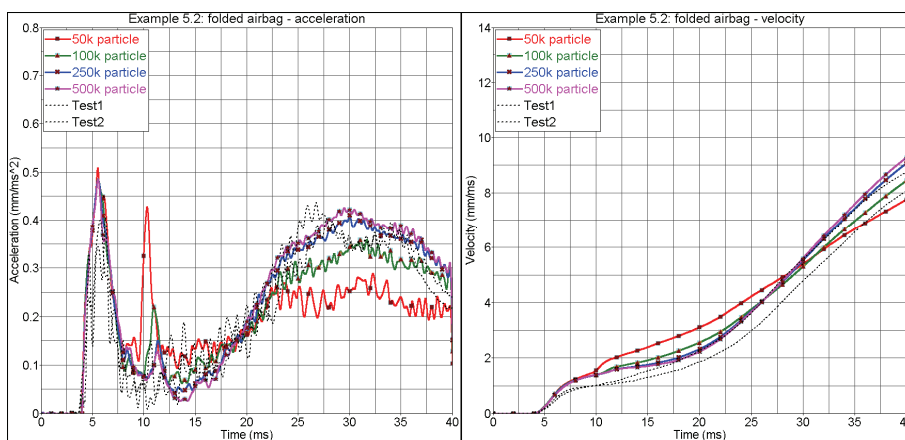


Figure 19: Acceleration and velocity of the semi-sphere for \*AIRBAG\_PARTICLE with different number of particles

Different Methods	No. of proc.	Elapsed time (sec)
*AIRBAG_HYBRID	1 SMP AMD 2.8GHz	11.175
*COMMON ALE 350.000 cells	1 SMP AMD 2.8GHz	169.590
*AIRBAG_PARTICLE 250.000 particle	1 SMP AMD 2.8GHz	31.308

Figure 20: Comparison of computing time for different models on one CPU

Different no. of particles	No. of proc.	Elapsed time (sec)
*AIRBAG_PARTICLE 50.000 particle	1 SMP AMD 2.8GHz	14.705
*AIRBAG_PARTICLE 100.000 particle	1 SMP AMD 2.8GHz	17.778
*AIRBAG_PARTICLE 250.000 particle	1 SMP AMD 2.8GHz	31.308
*AIRBAG_PARTICLE 500.000 particle	1 SMP AMD 2.8GHz	51.768

Figure 21: Convergence study of the C method

Different no. of processors	No. of proc.	Elapsed time (sec)
*AIRBAG_PARTICLE 250.000 particle	1 MPP AMD 2.0GHz	37.071
	2 MPP AMD 2.0GHz	30.357
	4 MPP AMD 2.0GHz	22.629
	8 MPP AMD 2.0GHz	32.123

Figure 22: Comparison of computing time for different models and number of processor

## 7 Summary

The corpuscular (C) method has proven to be a very promising new development path for airbag deployment simulations in LS-DYNA. In particular the application of the method is rather simple and straight forward. Switching from a \*AIRBAG\_HYBRID input deck towards \*AIRBAG\_PARTICLE is very easy and by no means as complicated as setting up an ALE input deck. The present examples show that the accuracy and agreement with experimental results of the new method are very good. Especially if complex folding in combination with wall-to-wall contact under high pressure is anticipated the method will become the method of choice. More over, if the flow needs to bend along sharp edges the new method is capable of capture the main effect with the same discretization while for ALE a much finer Eulerian mesh needs to be chosen. Last but not least a significant increase of speed for similar or better results has been found, i.e. the total simulation time is smaller.

Furthermore the set up and the validation of an airbag model are currently a very time and money consuming, tedious task. It seems that with \*AIRBAG\_PARTICLE a fast and accurate modelling technique for fluid-structure-interaction dominated problems is for the first time at hands. Particularly the validation process in order to gain predictable models can be shortened significantly.

However, prerequisites for predicable simulations are sufficiently fine and accurately meshed models. This holds also for additional model parts like tethers, vents and inflator geometry. Moreover, the constitutive description of the parts needs to be as accurate as possible. Again, a rigorous validation of the airbag fabric material as discussed in chapter 2 is of uttermost importance.

Further investigations on the new method to simulate vent holes, fabric porosity etc. will be done in the near future at DaimlerChrysler AG, Sindelfingen, Germany.

In addition to the present models new airbag designs for different applications like frontal impact (in and out of position) of driver, passenger and knee airbag as well as side impact investigations for sidebags and windowbags will be performed. Particularly for side impact simulations \*AIRBAG\_PARTICLE is interesting to be used in fully integrated models. Clearly, here a good performing MPP integration is necessary.

Last but not least post processing of the new method is not yet fully supported in LS-PrePost. Especially a feature to visualize pressure and flow on local basis is necessary to examine the particle flow in detail. The output of significant particle data in ABSTAT\_CPM is currently under way and will be released in the near future.

---

## 8 References

- [1] Beesten, B., Reilink, R., Hirth, A., Remensperger, R., Rieger, D., See, G. (2004): OOP Simulation – A Tool to Design Airbags? Current Capabilities in Numerical Simulation, *In: Airbag 2004, 7th International Symposium and Exhibition of Sophisticated Safety Systems, ISSN 0722-4087*, November 29 - December 1, 2004, Karlsruhe, Germany.
- [2] Haufe, A., Franz, U. (2004): On the Simulation of Out-of-Position Loadcases with the ALE-Method, *In: Airbag 2004, 7th International Symposium and Exhibition of Sophisticated Safety Systems, ISSN 0722-4087*, November 29 - December 1, 2004, Karlsruhe, Germany.
- [3] Haufe, A., Hallquist, J., Schweizerhof, Ka. (2005): Airbag Deployment in Out-of-Position Loadcases: A Challenging Fluid-Structure-Interaction Problem., *invited contribution to 5th International Conference on Computation of Shell and Spatial Structures, Ed: Ramm, Wall, Bletzinger & Bischoff*, June 1-4, Salzburg, Austria.
- [4] Hirth, A., Haufe, A. (2003), „ALE-Methode zur Airbagberechnung – Beispiele aus der Automobilindustrie“, LS-DYNA Update 2003, 11. November 2004, Stuttgart, Germany.
- [5] Marklund, P.-O., Nilsson, L. (2002), “Simulation of Airbag Deployment using a coupled Fluid-Structure Approach”, 7<sup>th</sup> International LS-DYNA Users Conference, 2002, Detroit, USA.
- [6] Olovsson, L. (2000) "On the Arbitrary Lagrangian-Eulerian Finite Element Method" Ph. D. Thesis, Linköping University.
- [7] Olovsson, L. (2003), „MAT\_GAS\_MIXTURE, a new gas mixture model for airbag applications“, 4<sup>th</sup> European LS-DYNA Users Conference, May 22-23, 2003, Ulm, Germany.
- [8] Olovsson, L. (2004) "ALE and Fluid Structure Interaction" Training class for LS-DYNA, DYNAmore GmbH, Stuttgart, Germany.
- [9] Wang, J. T., Nefske, D. J. (1988), "A new CAL3D Airbag Inflation Model" Int. Cong. Expo., SAE 880654, Detroit.

